Radiative recombination of bare ions with low-energy free electrons

M. Pajek* and R. Schuch
Manne Siegbahn Institute of Physics, S-104 05 Stockholm, Sweden
(Received 31 October 1991)

Radiative recombination of bare ions with electrons is discussed as a time-reversed photoionization process in the nonrelativistic dipole approximation. Analytical expressions for the radiative-recombination cross section and the angular distribution of the emitted photons are derived for an arbitrary (n,l) state in the low-energy limit. In this approximation, the anisotropy of the emitted photons is described by an *energy-independent* parameter β_{nl}. The radiative-recombination rate coefficients, both differential and angle integrated, for any (n,l) state can, in this limit, be expressed in analytical form. This result holds also for an anisotropic electron-velocity distribution characterized by a longitudinal $kT_{\parallel}$ and transverse $kT_{\perp}$ electron-beam temperatures. The results are discussed in context of the state-selective radiative-recombination experiments planned to be studied in electron coolers of heavy-ion storage rings.

PACS number(s): 34.80.Kw

I. INTRODUCTION

Radiative recombination is one of the fundamental processes in the electromagnetic interaction of charged particles. In this process, e.g., an ion captures a free electron and the excess energy is emitted as a photon. Radiative recombination is, essentially, a time-reversed photoionization process. The importance of radiative recombination has been recognized in many contexts such as plasma physics [1], astrophysics [2], and accelerator physics, in the last case for the process of cooling an ion beam in a storage ring with electrons [3].

The radiative recombination with particles other than electrons and ions, for example, muons (μ^-), positrons (e^+), or antiprotons ($\bar{p}$), has also been studied from the point of view of mesonic-atom physics [4], muon-catalyzed fusion [5], antihydrogen ($\bar{p}e^+$) production [6], and protonium ($p\bar{p}$) formation [7].

The heavy-ion storage rings (TSR [8], ESR [9], ASTRID [10], and CRYRING [11]) equipped with electron coolers offer unique possibilities to study radiative recombination between free electrons and bare or few-electron ions in much more detail. In this context, precision x-ray spectroscopy of H-like and few-electron ions via state-selective radiative recombination has been proposed [12,13].

The radiative-recombination process was studied theoretically, in the 1920s, by Kramers [14], Oppenheimer [15], Wessel [16], Stueckelberg and Morse [17], and by Stobbe [18], who gave the most extensive study of the subject. He derived, in the dipole approximation, the quantum-mechanical expression for the radiative-recombination cross section for arbitrary hydrogenic (n,l) states. Later, radiative recombination was discussed by Bethe and Salpeter [19], who derived a simple estimate of the radiative-recombination cross section for a fixed n state. Later the process was studied by several authors in the context of different experiments, namely, the muon (μ^-), pion (π^-), and kaon (K^-) radiative recombination by Baratella, Puddu, and Quarati [4] and the muon-catalyzed fusion process by Soff and Rafelski [5], who performed extensive numerical calculation of radiative-recombination cross sections. The process of antihydrogen production by induced radiative recombination, i.e., a photon-assisted radiative recombination of antiprotons ($\bar{p}$) with positrons (e^+), was discussed by Neumann *et al.* [6]. The question of protonium formation via radiative recombination between protons and antiprotons was discussed by Bracci, Fiorentini, and Pitzurra [7].

The radiative recombination between bare ions and free electrons, from the point of view of atomic physics experiments planned at heavy-ion storage rings, was discussed extensively by Liesen and Beyer [20] and Schuch *et al.* [21]. Also, the influence on the radiative-recombination process of the core electrons in not fully stripped ions (for energies relevant for plasma processes) was discussed by Hahn and Rule [22], Kim and Pratt [23], and, recently, by McLaughlin and Hahn [24].

Only recently have the first experimental results become available, both for the total radiative-recombination cross section (Andersen, Bolko, and Kvistgaard [25], Andersen and Bolko [26], and Müller *et al.* [27]) and for the state-selective laser-induced radiative-recombination process (Schramm *et al.* [28] and Yousif *et al.* [29]).

Since the radiative-recombination cross section increases with decreasing electron energy in the ionic system, this process gives the largest contribution for low relative energy. In fact, in many cases it is enough to know the recombination cross section in the limit of electron energy that is low relative to the electron binding energy in the final state. This condition is perfectly fulfilled for the electron-ion experiments planned in the storage rings. There, typically 0.2-eV electrons (transverse electron-beam temperature in an ion frame) recombine with a cooled beam of high-Z bare of few-electron ions, these having binding energies in the kilo-electron-volt

range for low (n,l) states.

The aim of this paper is to study systematically the state-selective radiative recombination of free electrons with bare ions in the low-energy limit. In this limit, we give compact analytical results for arbitrary (n,l) states for (i) electric dipole matrix elements, (ii) radiative-recombination cross sections, (iii) angular distributions of x rays and, finally, (iv) rate coefficients (double differential, differential, and integrated) for arbitrary electron-beam-velocity distribution characterized by longitudinal and transverse electron-beam temperatures, $kT_{\parallel}$ and $kT_{\perp}$, respectively.

II. RADIATIVE RECOMBINATION IN THE LOW ELECTRON ENERGY LIMIT

The radiative recombination of a free electron to the bound (n,l) state of a bare ion with atomic number Z may be written as

$$A^{Z+}+e^{-}\rightarrow A^{(Z-1)+}(n,l)+E_{\gamma}\ , \tag{1}$$

where n and l are the main and orbital electron quantum numbers in the final hydrogenic (n,l) state, and $E_{\gamma}=E+E_{nl}$ is the emitted photon energy, which equals the kinetic energy E of the electron plus the electron binding energy E_{nl} in the final state.

Since the radiative recombination is a time-reversed photoionization process, and the cross sections for both processes are related via the principle of detailed balance [30], one can use the known results (see, e.g., Ref. [31]) for the differential photoionization cross section $d\sigma_{nl}^{\rm ph}(E_{\gamma})/d\Omega$ to get the differential cross section $d\sigma_{nl}(E)/d\Omega$ for radiative recombination. In fact, when an electron with momentum $\mathbf{p}$ recombines with a bare ion, and the emitted photon has the momentum $\hbar\mathbf{k}$ ($E_{\gamma}=\hbar kc$), one can write, for a fixed polarization state of the photon (i.e., the electric vector orientation), the following relation between the differential cross sections for both processes (see Ref. [30]):

$$\frac{d\sigma_{nl}(E)}{d\Omega}=\frac{(\hbar k)^2}{p^2}\frac{d\sigma_{nl}^{\rm ph}(E_{\gamma})}{d\Omega}\ . \tag{2}$$

The differential photoionization cross section (i.e., the angular distributions of photoelectrons) $d\sigma_{nl}^{\rm ph}(E_{\gamma})/d\Omega$ appearing in this equation were studied extensively in the context of photoabsorption and photoelectron spectroscopy [31,32]. Within a nonrelativistic treatment in the dipole approximation the differential photoionization cross section can be expressed as follows [31]:

$$\frac{d\sigma_{nl}^{\rm ph}(E_{\gamma})}{d\Omega}=\frac{\sigma_{nl}^{\rm ph}(E_{\gamma})}{4\pi}\left[1+\frac{\beta_{nl}(E_{\gamma})}{2}[3(\mathbf{e}\cdot\mathbf{u}_p)^2-1]\right], \tag{3}$$

where $\sigma_{nl}^{\rm ph}(E_{\gamma})$ is a total (angle-integrated) photoionization cross section and $\mathbf{u}_p$ and $\mathbf{e}$ are unit vectors directed along the electron momentum and photon electric vector, respectively. $\beta_{nl}(E_{\gamma})$ is the so-called anisotropy parameter [31], describing completely the angular distribution of photoelectrons. In the dipole approximation, the quantities $\sigma_{nl}^{\rm ph}(E_{\gamma})$ and $\beta_{nl}(E_{\gamma})$ in Eq. (3) can be expressed [31] in terms of the electric dipole matrix elements $d_{l\pm1}(E_{\gamma})$, as will be discussed in detail in the following sections.

Finally, taking into account that the total (angle-integrated) cross sections for radiative recombination $\sigma_{nl}(E)$ and photoionization $\sigma_{nl}^{\rm ph}(E_{\gamma})$ are related in the same way as the corresponding differential cross sections [30], namely, $\sigma_{nl}(E)=[(\hbar k)^2/p^2]\sigma_{nl}^{\rm ph}(E_{\gamma})$, it turns out that the same relation as Eq. (3) holds for the differential radiative-recombination cross section:

$$\frac{d\sigma_{nl}(E)}{d\Omega}=\frac{\sigma_{nl}(E)}{4\pi}\left[1+\frac{\beta_{nl}(E)}{2}[3(\mathbf{e}\cdot\mathbf{u}_p)^2-1]\right]. \tag{4}$$

Throughout this paper we will use the fact that the differential radiative-recombination cross section can be described completely by the total recombination cross section $\sigma_{nl}(E)$ and anisotropy parameter $\beta_{nl}(E)$, which in turn are expressed by the electric dipole matrix elements [31]. In the following sections we will discuss in detail the $\sigma_{nl}(E)$ cross section and anisotropy parameter $\beta_{nl}(E)$ for the case of low electron energy $E\ll E_{nl}$. In this limit, both the radiative-recombination cross section and rate coefficient can be expressed analytically.

In the present paper the radiative recombination is discussed within a nonrelativistic dipole approximation [18,19,31]. A recent justification of this approach for low-energy electrons ($E\ll E_{nl}$) can be found in a publication by Scofield [33], who discussed, in a relativistic treatment including higher multipoles, the angular distribution of photons from radiative recombination with keV electrons. He showed that a nonrelativistic dipole approximation describes the recombination process very well for electron energies in the eV region. Generally, an influence of the relativistic effects on the radiative recombination can be discussed in light of existing extensive studies [34,35] of a time-reversed photoionization process, which is described by the same matrix elements for the bound-continuum transitions. For total K-shell photoelectric cross sections it was established long ago by Hall [34] that the relativistic effects are not important in photoelectric process even for the heaviest elements, where $\alpha Z\approx0.6$, unless the photoelectron energy is higher than the electron binding energy, namely, when $E\leq E_{nl}$. To be more precise, we have compared a nonrelativistic K-shell photoionization cross section for uranium ($Z=92$) as given in the dipole approximation by Stobbe [18] with the existing relativistic calculations, including higher multipoles, of Hultberg, Nagel, and Olsson [38]. In these calculations the relativistic unscreened Dirac wave functions were used, which makes these results especially suited for describing recombination of bare ions, where a hydrogenlike system is the final state. For the lowest available photon-energy point for uranium $E_{\gamma}=132$ keV, corresponding to $E/E_K\approx0.15$, we found an excellent agreement (within 1.2%) for both approaches, indicating that a nonrelativistic dipole approximation can be used safely even for high nuclear charges in the low-energy regime. Despite the observation that the relativistic effects do not influence strongly the total photoionization cross sections when $E\ll E_{nl}$, it

was found [32,36,37] that the anisotropy parameter β_{nl} is much more sensitive on relativistic corrections. Detailed discussion of this question for different (n,l) states was given by Pratt and co-workers [36,37] and Manson and Starace [32], where the general conclusion was drawn that a nonrelativistic dipole approximation describes the β_{nl} parameter fairly well for *inner* shells ($n<4$), but for *outer* shells in many-electron atoms strong relativistic effects related to the, so-called, Cooper minima (see Refs. [39] and [40]) were found. However, since these effects were found to be caused by a nonhydrogenic behavior [39,40] of the electronic wave functions, one can expect that it has less importance for a hydrogenlike ion (final state) discussed in the present paper. In fact, it was proved [40] that for one-electron ions treated nonrelativistically, due to a pure Coulomb potential, the Cooper minima do not occur at all. Summarizing, a nonrelativistic dipole approximation for radiative recombination between bare ions and free electrons is expected to be valid even for the highest nuclear charges in the discussed low-energy approximation $E \ll E_{nl}$.

A. Recombination cross section $\sigma_{nl}(E)$

For radiative recombination of bare ions with free electrons, both the initial- (continuum-) and final- (bound-) state wave functions are known analytically for any (n,l) state. Consequently, according to Stobbe [18], the radiative-recombination cross section σ_{nl}, within a nonrelativistic treatment in the dipole approximation, can be expressed as follows:

$$\sigma_{nl}(x)=\frac{\pi^2}{3}\alpha^3 a_0^2\frac{(1+x^2)^3}{x^3}[(l+1)|C_{nl}^{E,l+1}(x)|^2 + l|C_{nl}^{E,l-1}(x)|^2], \quad (5)$$

where $x=(E/E_{nl})^{1/2}$ is a dimensionless parameter which measures the free-electron kinetic energy relative to the electron binding energy in the final state, α is the fine-structure constant, and a_0 is the Bohr radius. The $C_{n,l}^{E,l\pm1}(x)$ are the electric dipole matrix elements [18] for transitions $[(E,l\pm1)\rightarrow(n,l)]$, which can be expressed in terms of parameter x (to get dimensionless quantities) as follows:

$$C_{nl}^{E,l+1}(x)=\frac{(-1)^{n_r}i}{8x^{3/2}(2l+1)!}\left[\frac{2\prod_{s=1}^{l+1}[s^2+(n/x)^2]}{\sinh\frac{n\pi}{x}}\right]^{1/2}\left[\frac{(n+l)!}{(n-l-1)!}\right]^{1/2}\exp\left[\left[\frac{\pi}{2}-2\arctan x\right]\frac{n}{x}\right]\left[\frac{4x}{1+x^2}\right]^{l+2}u^{n_r-1}$$
$$\times\left[{}_2F_1\left[l+2-i\frac{n}{x},-n_r,2l+2;1-\frac{1}{u^2}\right]-u^2\,{}_2F_1\left[l-i\frac{n}{x},-n_r,2l+2;1-\frac{1}{u^2}\right]\right] \quad (6)$$

and

$$C_{nl}^{E,l-1}(x)=\frac{(-1)^{n_r+1}}{8x^{3/2}(2l-1)!}\left[\frac{2\prod_{s=1}^{l-1}[s^2+(n/x)^2]}{\sinh\frac{n\pi}{x}}\right]^{1/2}\left[\frac{(n+l)!}{(n-l-1)!}\right]^{1/2}\exp\left[\left[\frac{\pi}{2}-2\arctan x\right]\frac{n}{x}\right]\left[\frac{4x}{1+x^2}\right]^{l+1}u^{n_r}$$
$$\times\left[{}_2F_1\left[l-i\frac{n}{x},-n_r,2l;1-\frac{1}{u^2}\right]-u^2\,{}_2F_1\left[l-i\frac{n}{x},-n_r-2,2l;1-\frac{1}{u^2}\right]\right], \quad (7)$$

where $n_r=n-l-1$, $u=(1+ix)/(1-ix)$, and ${}_2F_1(\alpha,\beta,\gamma;z)$ is the hypergeometric function [41]. Numerical calculations of the radiative-recombination cross section according to these rather complicated expressions were performed by Stobbe [18], Baratella, Puddu, and Quarati [4], Soff and Rafelski [5], and recently by Andersen and Bolko [26].

However, when the electron kinetic energy is much smaller than the binding energy of the electron in the final state, i.e, when $x \ll 1$, we show (see Appendix) that the electric dipole matrix elements in this limit depend on x in a much simpler way:

$$C_{nl}^{E,l+1}(x)\approx(-1)^{n-l-1}\frac{2^{2l+4}n^{l+1}e^{-2n}}{(2l+1)!}\left[\frac{(n+l)!}{(n-l-1)!}\right]^{1/2}$$
$$\times\left[F(l-n+1,2l+2;4n)-\frac{l-n+1}{l+1}F(l-n+2,2l+3;4n)\right]\sqrt{x}$$
$$=(-1)^{n-l-1}c_{l+1}(n,l)\sqrt{x} \quad (8)$$

and

$$C_{nl}^{E,l-1}(x)\approx(-1)^{n-l}\frac{2^{2l}n^{l-1}e^{-2n}}{(2l-1)!}\left[\frac{(n+l)!}{(n-l-1)!}\right]^{1/2}\times[F(l-n+1,2l;4n)-F(l-n-1,2l;4n)]\sqrt{x}=(-1)^{n-l}c_{l-1}(n,l)\sqrt{x}\ , \quad (9)$$

where we have introduced the *energy-independent* reduced electric dipole matrix elements $c_{l\pm1}(n,l)$. Here $F(\beta,\gamma;z)$ denotes the confluent hypergeometric function [41]. Since the parameter β in our case always is a nonpositive integer [see Eqs. (8) and (9)], the confluent hypergeometric function has a simple polynomial form (see Appendix).

Inserting the asymptotic expressions for the electric dipole matrix elements when $x \ll 1$ [Eqs. (8) and (9)] in Eq. (5), we find the following expression for the radiative-recombination cross section into the (n,l) state in the limit of low electron velocity:

$$\sigma_{nl}(x)\approx\frac{\pi^2}{3}\alpha^3a_0^2[(l+1)c_{l+1}^2(n,l)+lc_{l-1}^2(n,l)]\frac{1}{x^2}\ . \quad (10)$$

Equation (10) shows the well-known result that in the low-energy limit the radiative-recombination cross section scales as $1/E$ (since $x^2=E/E_{nl}$), and gives a simple analytical result for a fixed *arbitrary* (n,l) state:

$$\sigma_{nl}(E)\approx\frac{E_{nl}}{E}\sigma(n,l)\ , \quad (11)$$

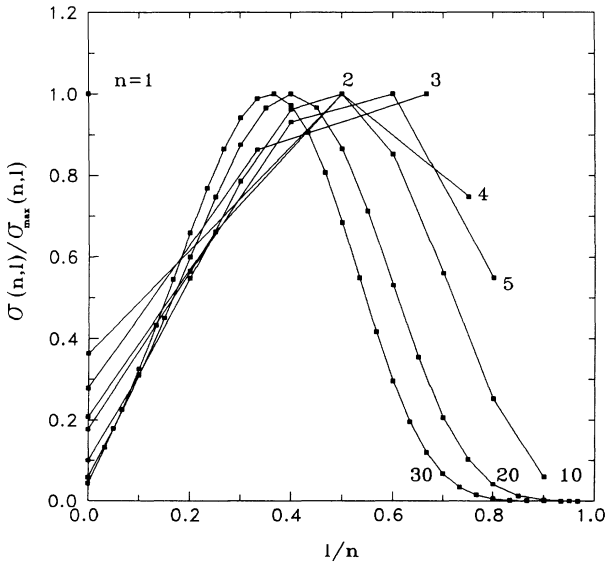

FIG. 1. Relative l distributions of the reduced recombination cross section, shown as the ratio of $\sigma(n,l)/\sigma_{\max}(n,l)$, where $\sigma_{\max}(n,l)$ denotes the largest $\sigma(n,l)$ cross section for a fixed n, vs the l/n ratio for selected n states with $n\leq30$. Note that for increasing n the curves approach a universal curve peaked at $l\approx n/3$.

where we have introduced the *reduced* radiative recombination cross section $\sigma(n,l)$:

$$\sigma(n,l)=\frac{\pi^2}{3}\alpha^3a_0^2[(l+1)c_{l+1}^2(n,l)+lc_{l-1}^2(n,l)]\ . \quad (12)$$

We point out that our simple analytical expression for the radiative-recombination cross section for an arbitrary (n,l) state contains information about the different l-state distributions, thus extending the widely used Bethe and Salpeter [19] formula which gives information only on the n-state distribution. Equation (11) also shows that the relative population of different l states in radiative recombination does not depend on electron energy in the low-energy limit. Numerically we found it to be approximately universal with respect to l/n. In Fig. 1, the relative population of different l states, $\sigma(n,l)/\sigma_{\max}(n,l)$ [where $\sigma_{\max}(n,l)$ means the largest cross section with respect to l for a fixed n], are shown for selected $n\leq30$ versus l/n. For the lowest n states this distribution peaks at $l\approx n/2$ and with increasing n it gets a more universal shape, with a maximum located at $l\approx n/3$.

The knowledge of the reduced radiative-recombination cross section [Eq. (12)] allows one to calculate the recombination cross section for any system (e.g., electron-ion, muon-ion, etc.), within the limit of low energy, using the scaling relation of Eq. (11). The numerical values of the reduced recombination cross section, for final states with $n\leq10$, are summarized in Table I. We should also mention here that the low-energy approximation discussed above was the subject of investigation in a few previously published papers. Stueckelberg and Morse [17] gave, we believe, the first correct result in the low-energy limit, but their analytical expressions are much more complicated than ours. Stobbe [18], despite the general formula for radiative-recombination cross section [Eq. (5)], gave closed analytical expressions only for the lowest $n=1$, 2, and 3 states. Radiative recombination in the low-energy limit was also investigated by Baratella, Puddu, and Quarati [4], but we believe that their final formula [Eq. (27) in Ref. [4]] is wrong. Finally, Andersen and Bolko [26] performed extensive numerical calculations which, due to the approximation used (only linear terms in the hypergeometric functions were taken into account), yield the same results as ours, but they did not get an analytical expression for the cross section.

B. Photon angular distribution $(d\sigma_{nl}/d\Omega)(\vartheta)$

In the introduction to Sec. II we have shown that the differential radiative-recombination cross section $d\sigma_{nl}(E)/d\Omega$, for a fixed polarization state of the photon, can be expressed by Eq. (4). However, when the polarization of the photons is not measured, one has to average the angle-differential cross sections [Eq. (4)] with respect to different polarization states (**e** directions) of the photons, measured at a fixed angle ϑ relative to the electron momentum direction. After such an averaging, the angular distribution of photons from radiative recombination, in polarization-insensitive experiments, may be expressed as follows:

TABLE I. The reduced radiative-recombination cross section $\sigma(n,l)$ (in barns), the ratio of the reduced electric dipole matrix elements $|c_{l-1}(n,l)/c_{l+1}(n,l)|$, and the anisotropy parameter β_{nl} for different (n,l) states, as obtained in the low-energy approximation $E \ll E_{nl}$. Note that for $l=0$ only $(E,l+1)\rightarrow(n,l)$ transitions contribute.

State (n,l)	$\sigma(n,l)$	$\left\lvert\frac{c_{l-1}(n,l)}{c_{l+1}(n,l)}\right\rvert$	β_{nl}
1 0	167.9		2.000
2 0	98.38		2.000
2 1	270.5	0.250	1.455
3 0	74.50		2.000
3 1	231.1	0.333	1.579
3 2	267.6	0.167	1.182
4 0	62.08		2.000
4 1	196.8	0.396	1.662
4 2	297.6	0.219	1.290
4 3	222.3	0.125	1.027
5 0	54.31		2.000
5 1	172.6	0.445	1.719
5 2	284.7	0.264	1.378
5 3	305.6	0.160	1.110
5 4	167.9	0.100	0.929
6 0	48.93		2.000
6 1	155.0	0.484	1.762
6 2	265.1	0.303	1.450
6 3	328.1	0.192	1.184
6 4	275.4	0.125	0.992
6 5	119.4	0.083	0.861
7 0	44.94		2.000
7 1	141.8	0.517	1.794
7 2	246.3	0.337	1.509
7 3	327.2	0.222	1.249
7 4	329.8	0.149	1.051
7 5	227.8	0.102	0.910
7 6	81.41	0.071	0.811
8 0	41.85		2.000
8 1	131.5	0.545	1.820
8 2	230.0	0.367	1.558
8 3	317.6	0.249	1.307
8 4	353.2	0.172	1.106
8 5	301.7	0.120	0.958
8 6	177.2	0.086	0.850
8 7	53.83	0.063	0.774
9 0	39.35		2.000
9 1	123.2	0.569	1.840
9 2	216.0	0.393	1.599
9 3	305.1	0.274	1.359
9 4	360.0	0.193	1.158
9 5	346.9	0.138	1.003
9 6	257.6	0.100	0.889
9 7	131.6	0.074	0.805
9 8	34.77	0.056	0.744

TABLE I. (*Continued*)

State (n,l)	$\sigma(n,l)$	$\left\lvert\frac{c_{l-1}(n,l)}{c_{l+1}(n,l)}\right\rvert$	β_{nl}
10 0	37.29		2.000
10 1	116.3	0.590	1.857
10 2	204.0	0.417	1.635
10 3	292.2	0.297	1.404
10 4	358.1	0.214	1.205
10 5	372.2	0.156	1.047
10 6	317.2	0.115	0.927
10 7	208.7	0.086	0.837
10 8	94.38	0.065	0.770
10 9	22.04	0.050	0.720

$$\frac{d\sigma_{nl}(E,\vartheta)}{d\Omega}=\frac{\sigma_{nl}(E)}{4\pi}\left[1-\frac{\beta_{nl}(E)}{2}P_2(\cos\vartheta)\right], \tag{13}$$

where $P_2(\cos\vartheta)=\frac{1}{2}(3\cos^2\vartheta-1)$ is the Legendre polynomial of second order. The question of the polarization of photons from radiative recombination into different (n,l) states will be discussed elsewhere [42].

For radiative recombination of bare ions with free electrons (hydrogenic ion in the final state), treated in the dipole approximation, the anisotropy parameter has the following form [31]:

$$\beta_{nl}(E)=\frac{(l+2)|d_{l+1}|^2+(l-1)|d_{l-1}|^2+6\sqrt{l(l+1)}\,\mathrm{Re}(d_{l+1}\bar{d}_{l-1}e^{i(\delta_{l+1}-\delta_{l-1})})}{(2l+1)(|d_{l+1}|^2+|d_{l-1}|^2)}, \tag{14}$$

where $\delta_{l\pm1}$ are the Coulomb phase shifts and the matrix elements $d_{l\pm1}$ (see Ref. [31]) are related to Stobbe's matrix elements $C_{nl}^{E,l\pm1}(x)$ [Eqs. (6) and (7)] as follows:

$$d_{l+1}\propto(-1)^{l+1}\sqrt{l+1}\,C_{nl}^{E,l+1}(x), \tag{15}$$

$$d_{l-1}\propto(-1)^{l}\sqrt{l}\,C_{nl}^{E,l-1}(x). \tag{16}$$

Since $\beta_{nl}(E)$ depends only on a ratio of $d_{l\pm1}$ quantities, in these formulas, for simplicity, a constant factor was omitted. As we showed in the preceding section, in the low-energy limit ($x\ll1$) the matrix elements $C_{nl}^{E,l\pm1}(x)$ are proportional to $\sqrt{x}$ [Eqs. (8) and (9)]. Additionally, for hydrogenic ions the Coulomb phase-shift difference in Eq. (14) may be expressed as [31]

$$\delta_{l+1}-\delta_{l-1}=-\left[\arctan\left[\frac{Z}{(l+1)p}\right]+\arctan\frac{Z}{lp}\right], \tag{17}$$

where p denotes the electron momentum (in atomic units). Consequently, the Coulomb phase-shift difference $\delta_{l+1}-\delta_{l-1}\to-\pi$ for a low-energy electron ($x\to0$). Finally we thus find that in the low-energy limit the anisotropy parameter β_{nl} becomes *energy independent* and may be expressed by the reduced matrix elements $c_{l\pm1}(n,l)$:

$$\beta_{nl}=\frac{(l+2)(l+1)c_{l+1}^2(n,l)+l(l-1)c_{l-1}^2(n,l)-6l(l+1)c_{l+1}(n,l)c_{l-1}(n,l)}{(2l+1)[(l+1)c_{l+1}^2(n,l)+lc_{l-1}^2(n,l)]}. \tag{18}$$

In particular, it turns out from Eq. (18) that for recombination to s states ($l=0$) only the $(E,l+1)\to(n,l)$ transition contributes and consequently $\beta_{n0}=2$, which corresponds to the well-known result that the angular distribution of photons for recombination to the K shell is proportional to $\sin^2\vartheta$ Ref. [19]. Usually, the $(E,l+1)\to(n,l)$ transition dominates over the $(E,l-1)\to(n,l)$ one [see Eqs. (8) and (9) and Table I]. This means that $|c_{l+1}(n,l)|\gg|c_{l-1}(n,l)|$, and in this case $\beta_{nl}\simeq(l+2)/(2l+1)$ and approaches the limiting value $\frac{1}{2}$ for large l (see Table I). The angular distributions of photons for selected (n,l) states for $n\le3$ are presented in Fig. 2. One can see that the angular distributions for states with $l\ge1$ have nonzero values for $\vartheta=0°$ and 180°. This is a tendency that the angular distributions are getting more flat with increasing n and l values, when β_{nl} goes to $\frac{1}{2}$ (see Table I for the values of β_{nl}).

III. RADIATIVE RECOMBINATION RATE COEFFICIENTS

Under realistic experimental conditions, the electron beam in the electron cooler of a storage ring is characterized by effective longitudinal $kT_{\parallel}$ and transverse $kT_{\perp}$

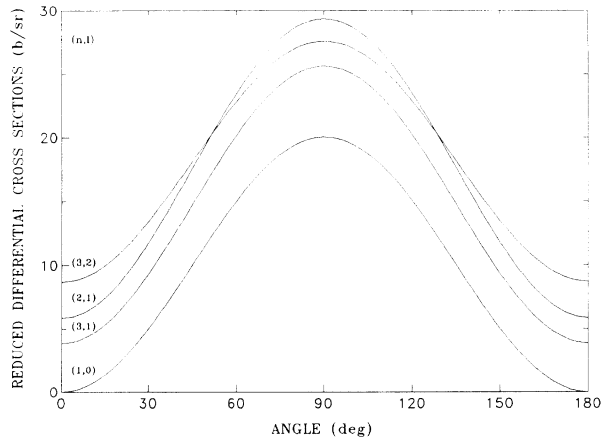

FIG. 2. Reduced angle-differential radiative-recombination cross sections $d\sigma(n,l)(\vartheta)/d\Omega=[\sigma(n,l)/4\pi][1-(\beta_{nl}/2)P_2(\cos\vartheta)]$ vs photon-emission angle ϑ (in the ion frame) for selected states (n,l) with $n\leq 3$. Note that for all $(n,0)$ states, $\beta_{n0}=2$, i.e., the angular dependencies are the same for these states.

beam temperatures and has, in the ion frame, the following relative velocity $[\mathbf{v}=(v_\parallel,v_\perp)]$ distribution [20,21]:

$$f(\mathbf{v})=\left[\frac{m}{2\pi}\right]^{3/2}\frac{1}{kT_\perp(kT_\parallel)^{1/2}}\exp\left[-\frac{mv_\perp^2}{2kT_\perp}-\frac{mv_\parallel^2}{2kT_\parallel}\right], \tag{19}$$

where m is the electron mass and k denotes the Boltzmann constant. In the electron cooler, the effective electron-beam temperatures in the ion frame ($kT_\parallel$ and $kT_\perp$) result from convolution of the electron- and ion-beam-velocity distributions, characterized by $(kT_{e\parallel},kT_{e\perp})$ and $(kT_{i\parallel},kT_{i\perp})$ beam temperatures, respectively. Consequently, one gets the following expression for the effective electron-beam temperature in the ion frame [20,21]:

$$kT_\parallel=kT_{e\parallel}+\frac{m}{M}kT_{i\parallel}, \tag{20}$$

$$kT_\perp=kT_{e\perp}+\frac{m}{M}kT_{i\perp}, \tag{21}$$

where m and M are the electron and ion masses, respectively. When the electron beam has some velocity distribution $f(\mathbf{v})$, instead of the radiative-recombination cross section defined for a fixed electron velocity [Eq. (5)], it is convenient to introduce the integrated quantity, the rate coefficient α_{nl}, defined as follows:

$$\alpha_{nl}=\langle v\sigma_{nl}(\mathbf{v})\rangle=\int v\sigma_{nl}(\mathbf{v})f(\mathbf{v})d^3\mathbf{v}. \tag{22}$$

In the same way, the double-differential $d^2\alpha_{nl}/dE_\gamma d\Omega$ and differential $d\alpha_{nl}/d\Omega$ rate coefficients can be introduced. In the low-energy electron limit ($x\ll 1$), the radiative-recombination rate coefficients can be expressed analytically for an arbitrary (n,l) state. This will be shown in the next subsections.

A. Double-differential $d^2\alpha_{nl}/dE_\gamma d\Omega$ rate coefficient

The double-differential $d^2\alpha_{nl}/dE_\gamma d\Omega$ rate coefficient is related to the differential radiative-recombination cross section [Eq. (13)] and the electron-beam-velocity distribution [Eq. (19)] in the following way [21]:

$$\frac{d^2\alpha_{nl}}{dE_\gamma d\Omega}=\frac{2(E_\gamma-E_{nl})}{m^2}\int\frac{d\sigma_{nl}}{d\Omega_r}(\mathbf{v})f(\mathbf{v})d\Omega_r, \tag{23}$$

where E_γ is the emitted photon energy, $d\Omega_r=\sin\vartheta d\vartheta d\varphi$ denotes the solid angle in the polar coordinates (ϑ,φ) defined by the momentum $\mathbf{p}$ of the incoming electron. In order to get the radiative-recombination rate coefficient for a fixed (in the ion frame) observation angle θ relative to the ion-beam direction, we have to perform an angular integration over $d\Omega_r$ in Eq. (23). Inserting the expression for the angle-differential radiative-recombination cross section $d\sigma_{nl}/d\Omega_r$ [Eq. (13)] with anisotropy parameter β_{nl} from Eq. (18) into Eq. (23) one obtains, following Liesen and Beyer [20], that the double-differential rate coefficient has the following form:

$$\frac{d^2\alpha_{nl}}{dE_\gamma d\Omega}(E_\gamma,\theta)=\frac{E_{nl}\sigma(n,l)}{\pi(2\pi m)^{1/2}}\frac{\exp[-(E_\gamma-E_{nl})/kT_\perp]}{kT_\perp(kT_\parallel)^{1/2}}\times\left[\left[1-\frac{\beta_{nl}}{2}\right]f_0(a)+\tfrac{3}{4}\beta_{nl}f_1(a)-\tfrac{3}{4}\beta_{nl}f_2(a)\sin^2\theta\right], \tag{24}$$

where the functions $f_i(a)$ are defined as follows:

$$f_0(a)=\int_0^1 e^{ax^2}dx, \tag{25}$$

$$f_1(a)=\int_0^1 e^{ax^2}(1-x^2)dx, \tag{26}$$

$$f_2(a)=\tfrac{1}{2}\int_0^1 e^{ax^2}(1-3x^2)dx, \tag{27}$$

with

$$a=(E_\gamma-E_{nl})\frac{kT_\parallel-kT_\perp}{kT_\parallel kT_\perp}. \tag{28}$$

For the case of recombination to the s state, the present results coincide with the expression for K shell given by Liesen and Beyer [20], being a specific case in our general result for $\beta_{10}=2$. In this context, it is worthwhile to note that in the previous study by Schuch *et al.* [21] it was assumed erroneously that the angular distribution of photons follows the $\sin^2\vartheta$ law for any (n,l) state. In light of Eq. (13), this is true only for the s states, where due to $\beta_{n0}=2$ one gets the $\sin^2\vartheta$ factor in the angular distribution.

We would like to point out that the double-differential rate coefficient for photon energies near the edge ($E_\gamma\approx E_{nl}$) does not depend on β_{nl} or θ, since for $a=0$ one has $f_0(0)=1$, $f_1(0)=\frac{2}{3}$, and $f_2(0)=0$. It can be written as

$$\frac{d^2\alpha_{nl}}{dE_\gamma d\Omega}(E_\gamma\approx E_{nl})=\frac{E_{nl}\sigma(n,l)}{\pi(2\pi m)^{1/2}}\frac{1}{kT_\perp(kT_\parallel)^{1/2}}, \tag{29}$$

which means that the magnitude of the sharp jump in the photon spectrum expected at $E_\gamma = E_{nl}$ [see Eq. (24); and Fig. 10 in Ref. [20]] will not be influenced by an x-ray anisotropy.

Finally, we would like to mention that while deriving Eq. (23) it was assumed that the width Γ_{nl} of the final state is small relative to the beam temperature $kT_\perp$ (see Ref. [21]). This assumption is exactly fulfilled for recombination into the ground state of the ion, which of course has a zero width. A possible modification of Eq. (23) for a nonzero width Γ_{nl} was studied by Schuch *et al.* [21], and will not be discussed here.

B. Angle-differential $d\alpha_{nl}/d\Omega$ rate coefficient

The angle-differential rate coefficient $d\alpha_{nl}/d\Omega$ can be obtained by integrating the double-differential rate coefficient $d^2\alpha_{nl}/dE_\gamma d\Omega$ [Eq. (24)] over the photon energy E_γ:

$$\frac{d\alpha_{nl}}{d\Omega}(\theta)=\int_{E_{nl}}^{\infty} dE_\gamma \frac{d^2\alpha_{nl}}{dE_\gamma d\Omega}(E_\gamma,\theta) . \tag{30}$$

Note that there is no contradiction in taking this integral up to infinity ($E_\gamma \to \infty$) within the low-energy approximation ($E \ll E_{nl}$) since the integral is, in a good approximation, mostly determined by the contribution around the end-point photon energies $E_\gamma \approx E_{nl}$. Before performing the integration in Eq. (30), we rewrite $d^2\alpha_{nl}(E_\gamma,\theta)/dE_\gamma d\Omega$ [Eq. (24)], introducing the full expressions for the $f_i(a)$ functions [Eqs. (25)–(27)] and variable $E = E_\gamma - E_{nl}$. From this we have

$$\frac{d^2\alpha_{nl}}{dE_\gamma d\Omega}(E,\theta)=\frac{E_{nl}\sigma(n,l)}{\pi(2\pi m)^{1/2}}\frac{1}{kT_\perp(kT_\parallel)^{1/2}}\int_0^1 dx[w_1(\theta)-w_2(\theta)x^2]\exp\left[-\left[\frac{1}{kT_\perp}+\frac{kT_\perp-kT_\parallel}{kT_\parallel kT_\perp}x^2\right]E\right] , \tag{31}$$

where

$$w_1(\theta)=1+\frac{\beta_{nl}}{4}-\tfrac{3}{8}\beta_{nl}\sin^2\theta , \tag{32}$$

$$w_2(\theta)=\tfrac{3}{4}\beta_{nl}(1-\tfrac{3}{2}\sin^2\theta) . \tag{33}$$

Now changing the integration variable in Eq. (30) from E_γ to $E = E_\gamma - E_{nl}$ we get

$$\frac{d\alpha_{nl}}{d\Omega}(\theta)=\frac{E_{nl}\sigma(n,l)}{\pi(2\pi m)^{1/2}}\frac{1}{kT_\perp(kT_\parallel)^{1/2}}\int_0^\infty dE\int_0^1 dx[w_1(\theta)-w_2(\theta)x^2]\exp\left[-\left[\frac{1}{kT_\perp}-\frac{kT_\perp-kT_\parallel}{kT_\parallel kT_\perp}x^2\right]E\right] . \tag{34}$$

Introducing in this integral a dimensionless parameter t,

$$t=\frac{kT_\perp-kT_\parallel}{kT_\parallel} , \tag{35}$$

which is a measure of the asymmetry of the electron-beam-velocity distribution, and changing the order of integration in Eq. (34) and introducing a new integration variable $w = E/kT_\perp$, we find

$$\frac{d\alpha_{nl}}{d\Omega}(\theta)=\frac{E_{nl}\sigma(n,l)}{\pi(2\pi m)^{1/2}}\frac{(t+1)^{1/2}}{(kT_\perp)^{1/2}}\times\int_0^1 dx[w_1(\theta)-w_2(\theta)x^2]\times\int_0^\infty dw\exp[-(1+tx^2)w] . \tag{36}$$

The integration over x and w in Eq. (36) can be performed analytically, and we arrive at the final result for the angle-differential rate coefficient:

$$\frac{d\alpha_{nl}}{d\Omega}(\theta)=\frac{E_{nl}\sigma(n,l)}{\pi(2\pi m)^{1/2}}\frac{1}{(kT_\perp)^{1/2}}(t+1)^{1/2}t^{-3/2}\times\{[w_1(\theta)t+w_2(\theta)]\times\arctan\sqrt{t}-w_2(\theta)\sqrt{t}\} . \tag{37}$$

This result shows that the angle-differential rate coefficient $d\alpha_{nl}(\theta)/d\Omega$ scales as $(kT_\perp)^{-1/2}$ times a function $G_{nl}(\theta,t)$ which depends only on an electron-beam asymmetry parameter t:

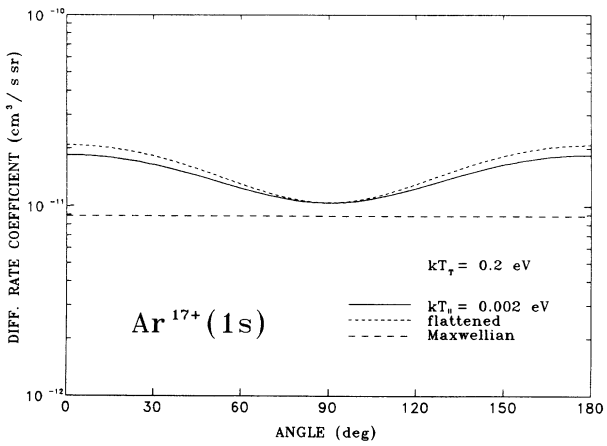

FIG. 3. Angle-differential rate coefficient $d\alpha_{nl}(\theta)/d\Omega$ for recombination of Ar^{18+} ions with electrons into the 1*s* state in Ar^{17+}, vs photon-emission angle θ in the ion frame. The electron beam is characterized by transverse temperature $kT_\perp = 0.2$ eV and different longitudinal temperatures $kT_\parallel$ as shown in the figure.

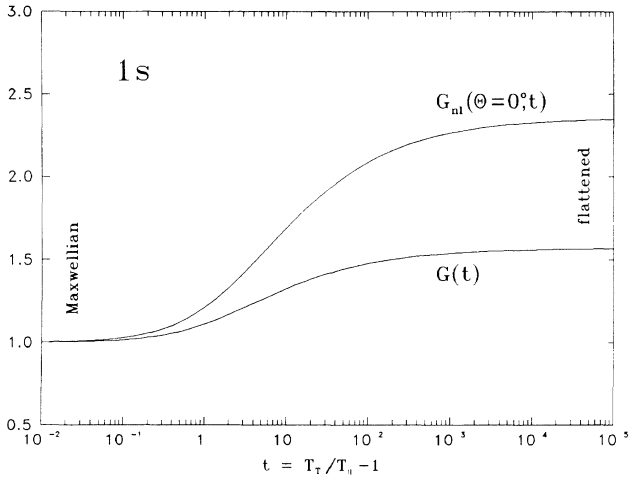

FIG. 4. Dependence of the $G_{nl}(\theta=0°;t)$ (shown for the $1s$ state) and $G(t)$ functions, see Eqs. (39) and (40), respectively, on the electron-beam asymmetry parameter $t=(kT_\perp - kT_\parallel)/kT_\parallel$. The extreme values of the asymmetry parameter t correspond to Maxwellian ($t\to 0$) and flattened ($t\to\infty$) electron-beam-velocity distributions.

$$G_{nl}(\theta,t)=(t+1)^{1/2}t^{-3/2}\{[w_1(\theta)t+w_2(\theta)] \times \arctan\sqrt{t} - w_2(\theta)\sqrt{t}\} . \quad (38)$$

In two extreme cases of the electron-beam-velocity distribution, namely, for Maxwellian ($kT_\parallel = kT_\perp; t\to 0$) and flattened ($kT_\parallel \ll kT_\perp; t\to\infty$) distributions, the values of the $G_{nl}(\theta,t)$ function approach $G_{nl}^{\mathrm{Max}}(\theta)=\frac{1}{3}[3w_1(\theta) - w_2(\theta)]$ and $G_{nl}^{\mathrm{flat}}(\theta)=(\pi/2)w_1(\theta)$, respectively. As an example, the angle-differential rate coefficient for the radiative recombination of low-energy electrons with Ar^{18+} ions (into the final $1s$ state) is shown in Fig. 3. An enhancement of the rate coefficients for forward and backward angles is clearly visible. It is also worthwhile to note that the angle-differential rate coefficient for $\theta=0°$, i.e., on the axis of the electron cooler, takes the following form:

$$G_{nl}(\theta=0°,t)=(t+1)^{1/2}t^{-3/2} \times \left\{ \left[\left[1+\frac{\beta_{nl}}{4} \right] t + \tfrac{3}{4}\beta_{nl} \right] \times \arctan\sqrt{t} - \tfrac{3}{4}\beta_{nl}\sqrt{t} \right\} . \quad (39)$$

This result shows immediately how a zero-degree x-ray measurement can be influenced by an x-ray anisotropy, described by the anisotropy parameter β_{nl} [Eq. (18)]. For Maxwellian and flattened electron-velocity distributions this function approaches $G_{nl}^{\mathrm{Max}}(\theta=0°;t\to 0)=1$ and $G_{nl}^{\mathrm{flat}}(\theta=0°;t\to\infty)=(\pi/2)(1+\beta_{nl}/4)$, respectively. The dependence of the $G_{nl}(\theta=0°,t)$ function on the electron-beam asymmetry parameter $t=(kT_\perp - kT_\parallel)/kT_\parallel$ is shown in Fig. 4. Note the essential increase of $d\alpha_{nl}/d\Omega(\theta=0°)$ by a factor of $(\pi/2)(1+\beta_{nl}/4)$ for a flattened electron-velocity distribution. Generally, this factor varies between $\frac{9}{16}\pi$ and $\frac{3}{4}\pi$ for the limiting β_{nl} values $\frac{1}{2}$ and 2, respectively (see Sec. II B and Table I).

C. Rate coefficient α_{nl}

The radiative-recombination rate coefficient α_{nl} can be derived by the angular integration of $d\alpha_{nl}/d\Omega$ [Eq. (37)]. The resulting expression is

$$\alpha_{nl}=\frac{4E_{nl}\sigma(n,l)}{(2\pi m)^{1/2}}\frac{1}{(kT_\perp)^{1/2}}\left[\frac{t+1}{t}\right]^{1/2}\arctan\sqrt{t} . \quad (40)$$

This equation contains a scaling function $G(t)=[(t+1)/t]^{1/2}\arctan\sqrt{t}$ which for extreme Maxwellian and flattened electron-velocity distributions approaches $G^{\mathrm{Max}}(t\to 0)=1$ and $G^{\mathrm{flat}}(t\to\infty)=\pi/2$, respectively. Also, Eq. (40) shows a well-known result [43], that the flattened electron-velocity distribution increases the rate coefficient by a factor of $\pi/2$ relative to the Maxwellian distribution. A dependence of the $G(t)$ function on the electron-beam asymmetry parameter t is shown in Fig. 4.

IV. DISCUSSION

Since the radiative-recombination cross sections and rate coefficients derived above were obtained in the low-energy approximation ($E \ll E_{nl}$) they are valid only up to some limiting $n_{\max}$ value. Indeed, setting the condition that a typical electron energy $E\approx kT_\perp \ll E_{nl}$, where $E_{nl}\approx Z^2E_0/n^2$ with $E_0=13.6$ eV being the Rydberg energy, one gets $n_{\max}\ll Z(E_0/kT_\perp)^{1/2}$. When we further assume that a typical value of the transverse electron-beam temperature in an electron cooler [3] is $kT_\perp\approx E_0/100$ we get $n_{\max}\ll 10Z$, which practically means that the low-energy approximation can be safely used up to $n_{\max}\approx Z$. This result shows that, for instance, for Ar^{18+} ions the low-energy approximation is valid for n states up to $n\approx 20$, or for U^{92+} ions up to $n\approx 100$. In this context, we cannot estimate the total radiative-recombination cross section, $\sigma_{\mathrm{tot}}(E)=\sum_{n=1}^{\infty}\sum_{l=0}^{n-1}\sigma_{nl}(E)$, and total rate coefficient, $\alpha_{\mathrm{tot}}=\sum_{n=1}^{\infty}\sum_{l=0}^{n-1}\alpha_{nl}$, within the low-energy approximation, which limits $n\le n_{\max}$. To calculate $\sigma_{nl}(E)$ and α_{nl} for $n>n_{\max}$ one has to go beyond the low-energy limit, but this question will be discussed separately [44].

In the following we will find a more quantitative condition for a validity of the low-energy approximation ($E\ll E_{nl}$) estimating how small $x=(E/E_{nl})^{1/2}$ should be to have an allowed accuracy of the analytical results, say ϵ. One finds that the next nonvanishing term in the expansion of Eq. (5) for small x, as compared to Eq. (10), is a quadratic one, namely $\sigma_{nl}(x)\approx(\sigma_{nl}/x^2)(1+\mathrm{const}\times x^2)$. By inspection of Eqs. (5)–(7) one finds that, roughly, $\mathrm{const}\approx n/3$, which gives us a simple estimation of the highest x value for an allowed accuracy as $nx^2/3\le\epsilon$. For instance, we see from this immediately that $x\le 0.3$ when 5% accuracy is desired for a recombination cross section into the ground

state. Furthermore, we can now relate n_{max} discussed above with an allowed degree of accuracy ϵ as follows: $n_{max} \leq (300\epsilon Z^2)^{1/3}$, for a typical electron-beam temperature $kT_\perp \approx E_0/100$ as above. One can thus find that the criterion established for the applicability of the low-energy approximation in the electron cooler, $n_{max} \leq Z$, corresponds, roughly, to an accuracy of 5% for Ar^{18+} and of 30% for U^{92+} ions.

Finally, it should be mentioned here that the results presented in previous sections for radiative-recombination cross sections, photon angular distributions, and rate coefficients are valid in the moving frame of the ion. The transformation from this frame to the laboratory system can be performed using the following relations [20]:

$$\cos\theta = \frac{\cos\theta_{lab} - \beta}{1 - \beta\cos\theta_{lab}} , \tag{41}$$

$$\frac{d\Omega}{d\Omega_{lab}} = \frac{1-\beta^2}{(1-\beta\cos\theta_{lab})^2} , \tag{42}$$

$$E_{\gamma,lab} = \frac{E_\gamma}{\gamma(1-\beta\cos\theta_{lab})} , \tag{43}$$

where $\beta = v_{ion}/c$, with v_{ion} being the ion velocity, $\gamma = 1/(1-\beta^2)^{1/2}$, and the index lab denotes the quantities in the laboratory system. The x-ray intensity measured on the axis of the electron cooler in the forward direction ($\theta_{lab} = 0°$) is increased due to this transformation by a factor $d\Omega(\theta = 0°)/d\Omega_{lab} = (1+\beta)/(1-\beta)$, which gives a 30% gain of x-ray intensity for the example of an Ar^{18+} ion beam with $\beta \approx 0.12$. The angle-differential recombination-rate coefficient $d\alpha_{nl}/d\Omega$ for this beam, transformed to the laboratory system, is shown in Fig. 5 for different longitudinal electron-beam temperatures. The advantage to using a forward angle to measure x rays from radiative recombination is evident in this figure. In fact, the ratio of angle-differential rate coefficients (in the laboratory system) for 0° and 180°, respectively, is $(1+\beta)^2/(1-\beta)^2$ according to Eqs. (41)–(43).

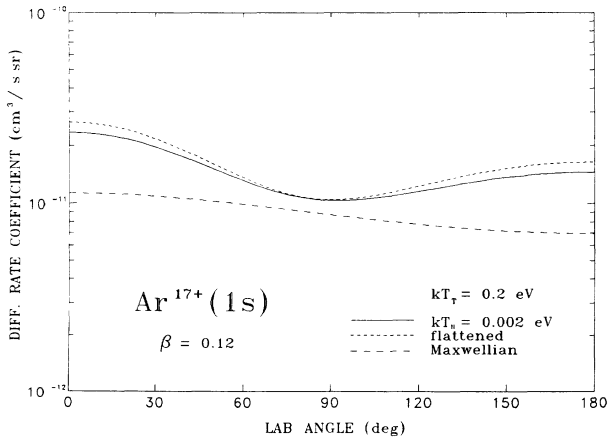

FIG. 5. The same rate coefficient as in Fig. 3, but after transformation to the laboratory system for an ion-beam velocity $\beta = 0.12$ and plotted vs photon observation angle θ_{lab}.

We find that the description of the radiative-recombination process within the low-energy approximation, valid for relatively high-n states with $n \leq Z$ and with most of the results having simple analytical form for arbitrary (n,l) states, offers a very convenient way to discuss state-selective radiative-recombination experiments proposed for heavy-ion storage rings [12,13].

V. CONCLUSIONS

In the present paper we have studied the radiative recombination of bare ions with free electrons in the low-energy limit $E \ll E_{nl}$, i.e., under conditions which are perfectly fulfilled in experiments planned to be performed in the electron coolers of storage rings. In this approximation, the electric dipole matrix elements have simple analytical forms. Moreover, we have also derived the analytical formulas for the state-selective radiative-recombination cross sections and angular distributions for an arbitrary (n,l) state. The rate coefficients can also be expressed analytically, for any electron-beam-velocity distribution, characterized by arbitrary longitudinal $kT_\parallel$ and transverse $kT_\perp$ beam temperatures. The results seem to be very useful for planning and analyzing the experiments concerning state-selective radiative recombination in the electron coolers of heavy-ion storage rings.

Note added in proof. When the present paper had been completed we learned about the paper by K. Omidvar and P. T. Guimaraes [Astrophys. J (Suppl. Ser.) **73**, 555 (1990)] where the oscillator strengths for hydrogenic bound-free transitions were discussed in the low-energy approximation. Analytical expressions obtained by these authors for the oscillator strengths in this approximation correspond to our expressions [Eqs. (A5)–(A8)] for the electric dipole matrix elements in the low-energy limit.

ACKNOWLEDGMENTS

We are grateful to Professor M. Ya. Amusia and Dr. A. Bárány for reading and discussing the manuscript.

APPENDIX

In this Appendix we find the asymptotic forms of Stobbe's [18] electric dipole matrix elements $C_{nl}^{E,l\pm1}(x)$ [Eqs. (6) and (7)] in the low-energy limit $E \ll E_{nl}$, i.e., for $x \ll 1$.

First of all we note that

$$\lim_{x\to 0} \frac{\exp[(\pi/2 - 2\arctan x)n/x]}{(\sin n\pi/x)^{1/2}} = \sqrt{2}e^{-2n} . \tag{A1}$$

Next, it is easy to show [41] that the hypergeometric functions appearing in Eqs. (6) and (7) have the following property:

$$\lim_{x\to 0} {}_2F_1\left[\alpha_i - i\frac{n}{x}, \beta_i, \gamma; \frac{4ix}{(1+ix)^2}\right] = F(\beta_i, \gamma; 4n) , \tag{A2}$$

where $F(\beta,\gamma;z)$ is the confluent hypergeometric function [41]. When the β parameter is a nonpositive integer, say $\beta = -m$, the confluent hypergeometric function can be

expressed [41] by a polynomial of order m:

$$F(-m,\gamma;z)=\sum_{k=0}^{m}\frac{(-m)_k}{(\gamma)_k}\frac{z^k}{k!}\ , \tag{A3}$$

where $(a)_k=a(a+1)\cdots(a+k-1)$.

We found, however, that an asymptotic form ($x\ll 1$) of the difference of hypergeometric functions ${}_2F_1(\ )-u^2(x){}_2F_1(\ )$ in Eqs. (6) and (7) depends on a relation between β's as follows:

$$ {}_2F_1\left[\alpha_1-i\frac{n}{x},\beta_1,\gamma;\frac{4ix}{(1+ix)^2}\right]-\left[\frac{1+ix}{1-ix}\right]^2{}_2F_1\left[\alpha_2-i\frac{n}{x},\beta_2,\gamma;\frac{4ix}{(1+ix)^2}\right] $$

$$ \underset{x\ll 1}{=}\begin{cases} F(\beta_1,\gamma;4n)-F(\beta_2,\gamma;4n), & \beta_1\neq\beta_2 \\ -4ix\left[F(\beta,\gamma;4n)-\dfrac{(\alpha_2-\alpha_1)\beta}{\gamma}F(\beta+1,\gamma+1;4n)\right], & \beta_1=\beta_2=\beta;\ \alpha_1\neq\alpha_2\ . \end{cases} \tag{A4}$$

With the help of Eqs. (A1) and (A4) it is easy to show that for $x\ll 1$

$$C_{nl}^{E,l+1}(x)\approx(-1)^{n-l-1}c_{l+1}(n,l)\sqrt{x}\ , \tag{A5}$$

$$C_{nl'}^{E,l-1}(x)\approx(-1)^{n-l}c_{l-1}(n,l)\sqrt{x}\ , \tag{A6}$$

where we have introduced the reduced electric dipole matrix elements $c_{l\pm1}(n,l)$, which do not depend on x. They have the following form:

$$c_{l+1}(n,l)=\frac{2^{2l+4}n^{l+1}e^{-2n}}{(2l+1)!}\left[\frac{(n+l)!}{(n-l-1)!}\right]^{1/2}\left[F(l-n+1,2l+2;4n)-\frac{l-n+1}{l+1}F(l-n+2,2l+3;4n)\right], \tag{A7}$$

$$c_{l-1}(n,l)=\frac{2^{2l}n^{l-1}e^{-2n}}{(2l-1)!}\left[\frac{(n-l)!}{(n-l-1)!}\right]^{1/2}[F(l-n+1,2l;4n)-F(l-n-1,2l;4n)]\ . \tag{A8}$$

In conclusion, we have shown that using Eqs. (A7) and (A8), with the help of Eq. (A3) to calculate the $F(\beta,\gamma;z)$ functions, the reduced electric dipole matrix elements $c_{l\pm1}(n,l)$ can easily be calculated analytically for arbitrary (n,l) states.

*Permanent address: Institute of Physics, Pedagogical University, 25-509 Kielce, Poland.

[1] *Atomic and Molecular Processes,* edited by D. R. Bates (Academic, New York, 1962).
[2] W. H. Tucker, *Radiation Processes in Astrophysics* (MIT University Press, Cambridge, MA, 1975).
[3] H. Poth, Phys. Rep **196**, 135 (1990).
[4] P. Baratella, G. Puddu, and P. Quarati, Z. Phys. A **300**, 263 (1981).
[5] G. Soff and J. Rafelski, Z. Phys. D **14**, 187 (1989).
[6] R. Neumann, H. Poth, A. Winnacker, and A. Wolf, Z. Phys. A **313**, 253 (1983).
[7] L. Bracci, G. Fiorentini, and O. Pitzurra, Phys. Lett. **85B**, 280 (1979).
[8] D. Habs *et al.*, Nucl. Instrum. Methods B **43**, 390 (1989).
[9] F. Bosch, Nucl. Instrum. Methods B **23**, 190 (1987).
[10] S. P. Møller, in *Proceedings of the European Particle Conference, Rome 1988* (World Scientific, Singapore, 1989), p. 112.
[11] K.-G. Rensfelt, in *IEEE-91 Particle Accelerator Conference,* edited by L. Lizama and J. Chew (IEEE Publishing Service, New York, 1991), Vol. 5, p. 2814.
[12] R. Schuch, Nucl. Instrum. Methods B **24/25**, 11 (1987).
[13] F. Bosch, Phys. Scr. **36**, 730 (1987).
[14] H. A. Kramers, Philos. Mag. **46**, 836 (1923).
[15] J. R. Oppenheimer, Phys. Rev. **31**, 349 (1928).
[16] W. Wessel, Ann. Phys. (Leipzig) **5**, 611 (1930).
[17] E. G. Stueckelberg and P. M. Morse, Phys. Rev. **36**, 16 (1930).
[18] M. Stobbe, Ann. Phys. (Leipzig) **7**, 661 (1930).
[19] H. Bethe and E. Salpeter, in *Quantum Mechanics of One- and Two-Electron Systems,* edited by S. Flügge, Handbuch der Physik Vol. 35 (Springer, Berlin, 1957).
[20] D. Liesen and H. F. Beyer, Gesellschaft für Schwerionenforschung Report (Darmstadt) No. GSI-ESR/86-04, 1986 (unpublished).
[21] R. Schuch, A. Bárány, H. Danared, N. Elander, and S. Mannervik, Nucl. Instrum. Methods B **43**, 411 (1989).
[22] Y. Hahn and D. W. Rule, J. Phys. B **10**, 2689 (1977).
[23] Y. S. Kim and R. H. Pratt, Phys. Rev. A **27**, 2913 (1983).
[24] D. J. McLaughlin and Y. Hahn, Phys. Rev. A **43**, 1313 (1991).
[25] L. H. Andersen, J. Bolko, and P. Kvistgaard, Phys. Rev. Lett. **64**, 729 (1990).
[26] L. H. Andersen and J. Bolko, Phys. Rev. A **42**, 1184 (1990); J. Phys. B **23**, 3167 (1990).
[27] A. Müller *et al.*, Phys. Scr. **T37**, 62 (1991).
[28] U. Schramm, J. Berger, M. Grieser, D. Habs, E. Jaeschke, G. Kilgus, D. Schwalm, A. Wolf, R. Neumann, and R. Schuch, Phys. Rev. Lett. **67**, 22 (1991).
[29] F. B. Yousif, P. Van der Donk, Z. Kucherovsky, J. Reis, E. Brannen, and J. B. A. Mitchell, Phys. Rev. Lett. **67**, 26 (1991).
[30] I. I. Sobelman, *Atomic Spectra and Radiative Transitions*

(Springer, Berlin, 1979).
[31] M. Ya. Amusia, *Atomic Photoeffect* (Plenum, New York, 1990).
[32] S. T. Manson and A. F. Starace, Rev. Mod. Phys. **54**, 389 (1982).
[33] J. H. Scofield, Phys. Rev. A **40**, 3054 (1989).
[34] H. Hall, Rev. Mod. Phys. **8**, 358 (1936).
[35] R. H. Pratt, A. Ron, and H. K. Tseng, Rev. Mod. Phys. **45**, 273 (1973).
[36] H. K. Tseng, R. H. Pratt, S. Yu, and A. Ron, Phys. Rev. A **17**, 1063 (1978).
[37] Y. S. Kim, R. H. Pratt, A. Ron, and H. K. Tseng, Phys. Rev. A **22**, 567 (1980).
[38] S. Hultberg, B. Nagel, and P. Olsson, Ark. Fys. **20**, 555 (1961); **38**, 1 (1968).
[39] S. Manson, Phys. Rev. A **31**, 3698 (1985).
[40] S. D. Oh and R. H. Pratt, Phys. Rev. A **34**, 2486 (1986).
[41] *Handbook of Mathematical Functions,* edited by M. Abramowitz and I. A. Stegun (Dover, New York, 1972).
[42] M. Pajek and R. Schuch (unpublished).
[43] M. Bell and J. S. Bell, Part. Accel. **12**, 49 (1982).
[44] M. Pajek and R. Schuch (unpublished).